

Circularly Polarized Antenna Array Fed by Substrate Integrated Waveguide: Implementation Recommendations

-

Dominika Warmowska, Zbyněk Raida

xwarmo00@stud.feec.vutbr.cz

Brno University of Technology, SIX Research Center

DOI: -

Abstract: In the paper, we review the design of a double-layered circularly polarized antenna array consisting of orthogonal linear antenna elements fed by substrate-integrated network. The reviewed array has been simulated in CST Microwave Studio, fabricated and measured. Based on the critical evaluation of obtained results, practical recommendations for the implementation of the numerical model and fabrication of the prototype of the antenna array have been compiled. Such a practical guide to the design of SIW-based millimeter-wave antenna arrays has not been published in the open literature yet.

Circularly Polarized Antenna Array Fed by Substrate Integrated Waveguide: Implementation Recommendations

Dominika Warmowska, Zbynek Raida

Brno University of Technology, SIX Research Center
Email: xwarwo00@stud.feec.vutbr.cz

Abstract – In the paper, we review the design of a double-layered circularly polarized antenna array consisting of orthogonal linear antenna elements fed by substrate-integrated network. The reviewed array has been simulated in CST Microwave Studio, fabricated and measured. Based on the critical evaluation of obtained results, practical recommendations for the implementation of the numerical model and fabrication of the prototype of the antenna array have been compiled. Such a practical guide to the design of SIW-based millimeter-wave antenna arrays has not been published in the open literature yet.

1 Introduction

Circularly polarized antennas have to be used to transmit and receive electromagnetic waves if the communication channel can influence polarization of the propagating wave. Such a situation is typical for satellite communication since the polarization can be rotated by atmospheric layers. Modern radar systems are another example of application [1].

If a sufficiently high gain of the antenna is requested to be achieved, several antenna elements have to be grouped into an array, and a proper feeding network has to be designed to ensure necessary amplitudes and phases of excitation currents at inputs of elements. For millimeter-wave frequencies and planar antennas, substrate integrated waveguides (SIW) can be used for the excitation to suppress parasitic radiation of the feeding network [2]–[3].

In order to radiate the circularly polarized wave, circular antenna elements can be used in the array, or orthogonal linear elements with proper phasing can be combined [4].

In [5], authors combined orthogonal linear radiators and the SIW feeding network to design a 4×4 antenna array operating with the axial ratio bandwidth 18.3 to 21.1 GHz and the gain higher than 13 dBi. The array was conceived as a double-layer structure with antenna radiators in the top layer and the SIW feeding network in the bottom layer.

Unfortunately, [5] did not include sufficient descriptions to make the design repeatable. Moreover, no sensitivity analysis and parametric study was provided to evaluate the influence of fabrication accuracy to final parameters of the implemented antenna.

In [6]–[8], design of a circularly polarized SIW antennas are discussed however none of them talks about the fabrication and implementation requirements of such antennas.

In this paper, practical aspects missing in [5]–[8] are presented. In Section 2, the design of SIW feeding structure is discussed, including the transition between the coaxial con-

ductor and SIW. Section 3 deals with the design of the array of orthogonal linear antenna elements, presents guidelines for an efficient simulation of the antenna array in CST Microwave Studio, and shows manufacturing problems and their possible solutions. Section 4 concludes the paper.

2 SIW feeding structure

Manufacturing of conventional waveguides is complicated and expensive, feeding networks are heavy and bulky. Microstrip transmission lines are of small dimensions but losses are significant at higher frequencies. Therefore, substrate integrated waveguides (SIW) have been introduced to solve the described problems [2], [3].

SIW is an equivalent of a rectangular waveguide. Top and bottom walls of the waveguide are created by the metallic layer covering both surfaces of a microwave substrate. Side walls of the waveguide are replaced by vias in a dielectric substrate (see Figure 1).

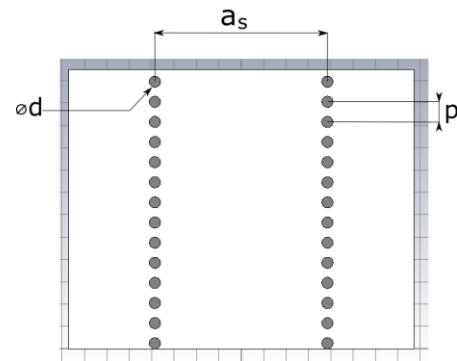


Figure 1: Substrate integrated waveguides (SIW).

The width of SIW [9]:

$$a_s = \frac{c}{2f\sqrt{\epsilon_r}} + \frac{d^2}{0.95p}, \quad (1)$$

differs from the width of the equivalent waveguide [9]:

$$a_w = \frac{c}{2f\sqrt{\epsilon_r}}. \quad (2)$$

Here, a_s is the width of the SIW with the TE₁₀ mode, a_w is the width of an equivalent waveguide filled in with the dielectric substrate with the dielectric constant ϵ_r , c is the speed of light

and f denotes the cut-off frequency. The distance between two neighboring vias is p , and the diameter of vias is d .

The distance between neighboring vias should not be too large to avoid leakage of electromagnetic energy out of the waveguide. The diameter of vias can be usually varied to respect limitations of the fabrication process.

Since the operation principle of a SIW is identical with a dielectric-filled waveguide, vias can be approximated by continuous metallic walls to reduce the number of mesh cells in the numerical model. Then, the field distribution in the waveguide can be calculated quickly.

For the feeding structure of the studied antenna array, both the SIW and the equivalent waveguide were designed using (1), (2) with the cutoff frequency $f = 15$ GHz. In Figure 2, frequency response of the transmission coefficient of the waveguide and SIW analyzed in CST Microwave Studio are presented. A good correlation between the transmission coefficients can be observed.

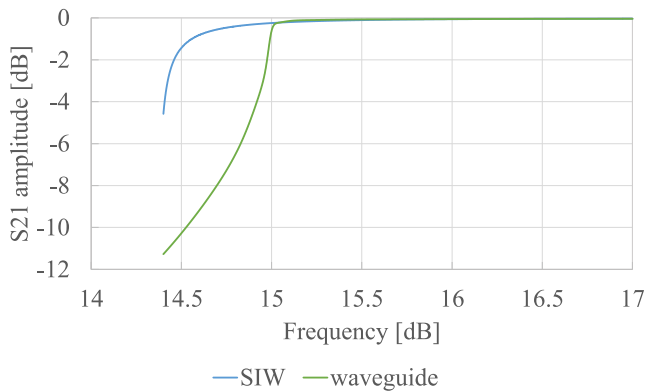


Figure 2: Frequency response of the transmission coefficient of SIW and equivalent waveguide.

In order to achieve circular polarization by orthogonal linear elements, the sequential rotation technique (SRT) was applied. Applying SRT, each antenna element is excited by uniform magnitude and progressive phase shift of 90° . Thanks to this technique, a wider axial ratio bandwidth can be achieved [4].

The studied antenna consists of two layers. The feeding system is integrated into the bottom layer, and an array of radiating elements is implemented in the upper layer [5].

The studied antenna array was designed to operate at the center frequency 20 GHz. The feeding network and the antenna array were designed and tuned separately to achieve SRT requirements.

The feeding network (Figure 3) consists of an input port (the port 1) and four feeding points transferring the signal to antenna elements in the upper layer. While analyzing the feeding system, feeding points are treated as ports 2 to 5.

Position of the metallic pins (parameters $n1$, $n23$, $n45$) influences the power division in a given ramification. For example, moving the metallic pin between the port 2 and 3 closer to the port 3 can result in higher power being received at the port 2. A different phase at each output port can be achieved by selecting a different distance between the input port to the output port. In the studied structure, the different distance is achieved by the N-shaped feeding with different lengths of

arms. Since the radiating part requires feeding points in a fixed position, lengths of arms should not be varied independently, and phase shifts could be tuned by widths of arms (parameters $w1$ to $w5$). The values of the parameters for the structure with 0.1 mm walls and for the structure with vias are presented in Table 1.

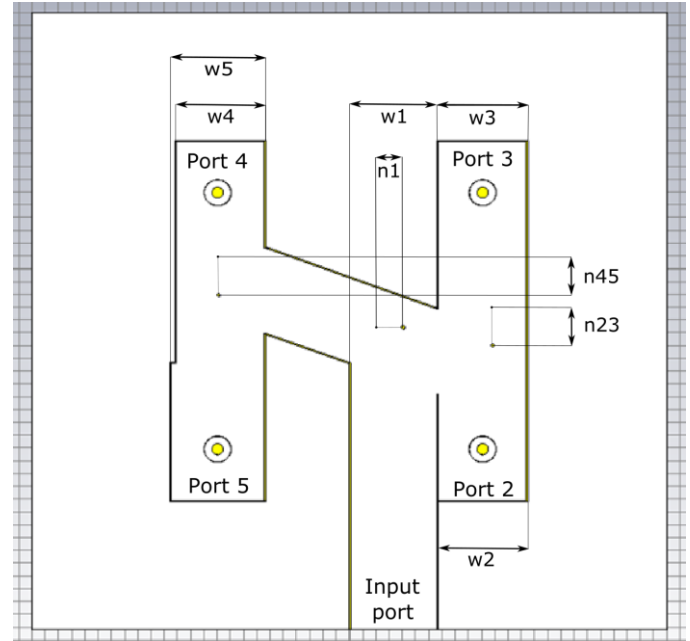


Figure 3: Structure of the feeding network.

Table 1: Dimensions of the feeding structure depicted in Figure 3: widths of waveguides $w1$ to $w5$, positions of vias $n1$, $n23$ and $n45$, all values are given in mm.

Parameter	Structure with 0.1 mm walls	Structure with vias
$w1$	6.64	6.90
$w2$	6.64	7.30
$w3$	6.64	7.20
$w4$	6.64	7.00
$w5$	7.04	7.20
$n1$	0.76	1.15
$n23$	0.47	0.60
$n45$	-0.36	-0.10

Feeding points of the antenna array are implemented in form of metal wires connecting the bottom ground layer and the top radiating part. Wires go through both the layers. In the analysis of the feeding structure, ports are defined between the wire (the inner conductor of a coaxial line) and the metal layer (the outer conductor of a coaxial line). A side cut of the port used in feeding structure analysis is shown in Figure 4.

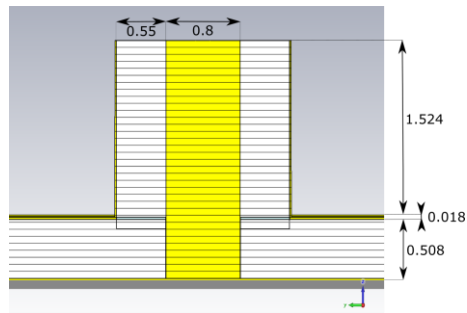


Figure 4: Side cut of port used for the analysis of the feeding structure. All dimensions are in mm.

In order to shorten the simulation time, side walls of SIW were approximated by PEC walls. First, the width of the wall was set to 0.1 mm and the structure was tuned to achieve results close to required ones.

Increasing the width of the wall to 0.5 mm, the transmission and reflection coefficients changed significantly (see Figure 5 and 6). This effect is caused by the internal wall between the input waveguide (the width w_1) and the branch 2 (the width w_2). Hence, the wall width has to be taken into account.

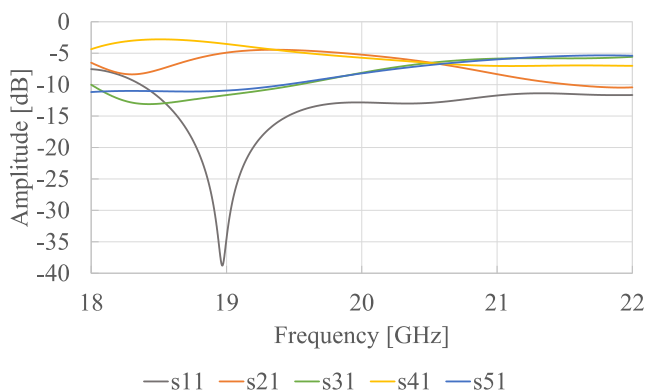


Figure 5: Frequency response of S-parameters of the feeding structure with 0.1 mm walls

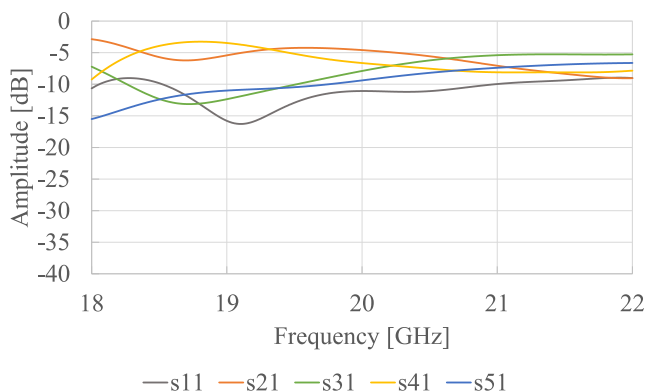


Figure 6: Frequency response of S-parameters of the equivalent feeding structure with 0.5 mm walls.

The available fabrication technology allows us to create vias with the diameter $d = 0.5$ mm. Therefore, the feeding network with thickness of walls 0.5 mm was tuned, and the

tuned network was transformed to SIW (the distance between vias $p = 0.9$ mm). A good agreement between the simulation with walls and vias was obtained considering power division (see Figure 7 and 8).

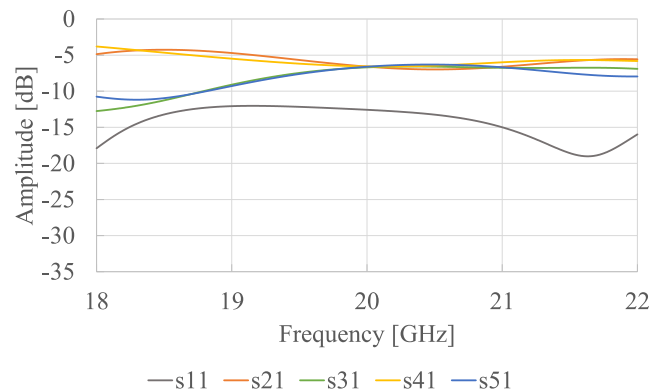


Figure 7: Frequency response of S-parameters of the feeding structure: 0.5 mm thick walls (after tuning).

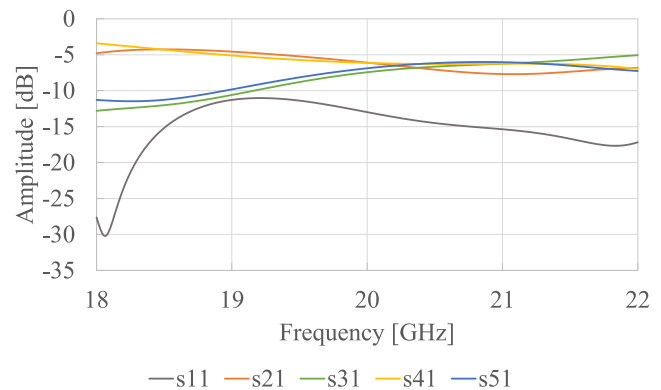


Figure 8: Frequency response of S-parameters of the SIW feeding structure with corresponding vias.

The feeding structure was tuned to achieve good impedance matching, equal power division and progressive phase shift. Fulfilling all these objectives is a complex, time consuming task, and therefore, we used a multi-objective optimization method called Non-Dominated Sorting Genetic Algorithm II (NSGA II). Optimization was implemented in MATLAB, and MATLAB was connected to the full-wave solver of CST Microwave Studio. Satisfying reflection and transmission coefficients together with good phase shifts were obtained. Details were presented in [10].

In order to make the model of the feeding network more realistic, the input port has to be connected to a coaxial connector using a tapered transmission line. The tapered line allows the impedance of a microstrip line or a coplanar waveguide (CPW) being transformed to the impedance of the SIW.

The basic microstrip-to-SIW transition structure was discussed in [11] and is presented in Figure 9. Unfortunately, this transition might be problematic when operated at higher frequencies. In that case, exploitation of CPW-to-SIW transition [12] is recommended (see Figure 10).

Designing the CPW-to-SIW transition, the length of the transition [12]:

$$L = \frac{n \lambda_g}{4}, \quad n = 1, 2, 3, \dots, \quad (3)$$

belongs to most important parameter of the taper. In (3), λ_g denotes the wavelength in a dielectric-filled waveguide.

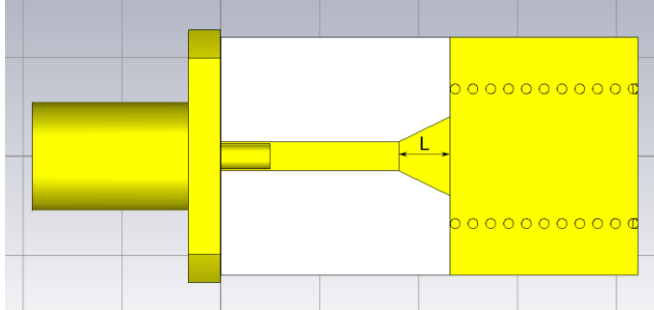


Figure 9: Microstrip transition between the coaxial connector and SIW.

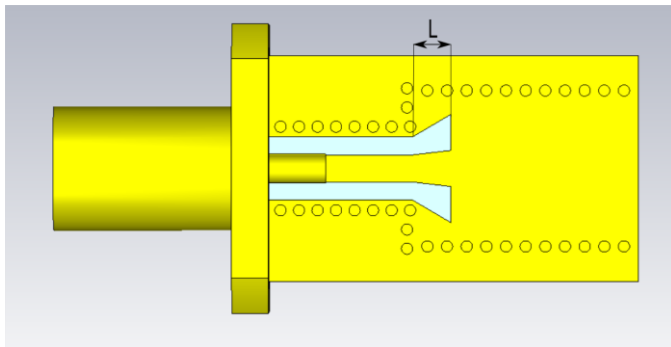


Figure 10: Coplanar waveguide transition between the coaxial connector and SIW.

Both the microstrip-to-SIW and CPW-to-SIW were modelled and analyzed in CST Microwave Studio. Frequency response of the transmission coefficient and the reflection coefficients are presented in Figure 11 and 12. Obviously, microstrip-to-SIW transition shows a significantly narrower bandwidth (2.2 GHz) compared to CPW-to-SIW transition (5.9 GHz). Therefore, the CPW-to-SIW transition was chosen for the implementation.

3 Antenna array

Radiating part of the antenna array in the top layer (above the feeding network) is divided into four sub-arrays consisting of four linearly polarized radiation slots. Feeding points are located in the center of each sub-array exactly. Each sub-array is excited by the signal of same amplitude and progressive phase. A proper field distribution is ensured by walls inside sub-arrays. The antenna layout is shown in Figure 13.

Performing parametric analysis of the antenna, we have varied the length of the radiating slot L_s , the width of the radiating slot W_s , the shift of the slots from the center position S , and gap between the feeding point and the wall inside the sub-array F .

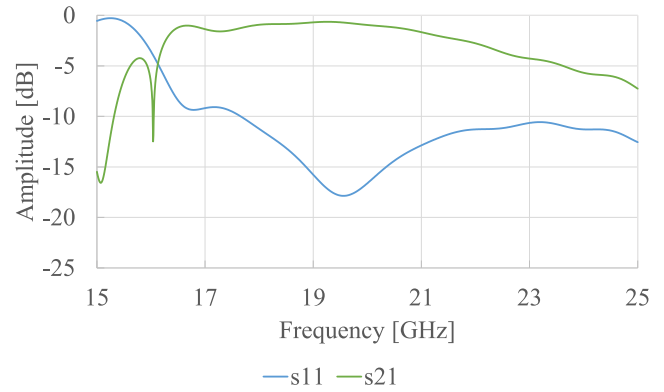


Figure 11: Frequency response of S-parameters of coaxial-to-SIW transition: microstrip taper (top)

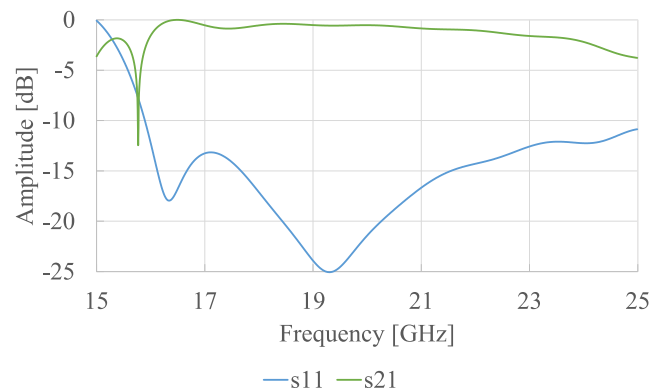


Figure 12: Frequency response of S-parameters of coplanar waveguide taper (bottom).

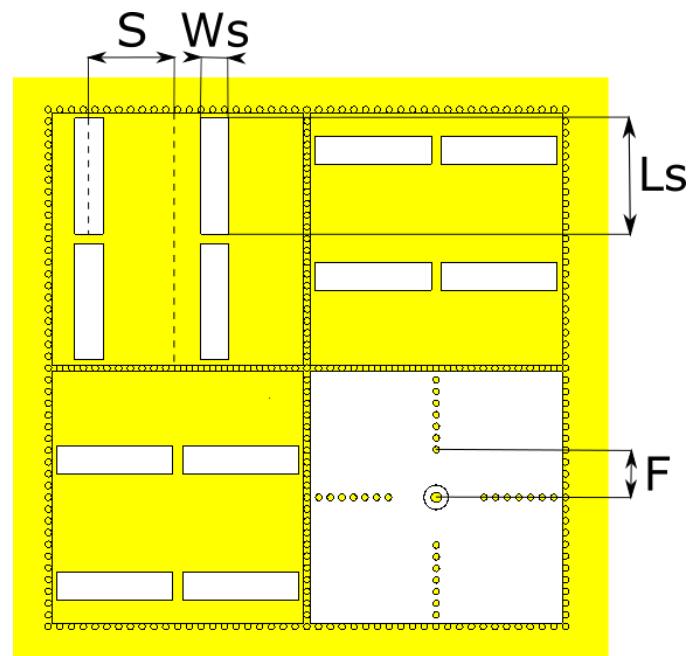


Figure 13: Layout of the radiation part of the antenna (metallization in lower-left corner is hidden to show inside SIW walls of subarrays).

Following conclusions can be formulated:

- The length of the slot influences the resonant frequency mostly.
- All parameters highly influence the axial ratio, and therefore need to be in a good agreement for satisfactory results. Since dependencies are straightforward, the CST build-in optimizer was used to optimize the radiating structure.

Table 2 : Dimensions of the radiation part of the antenna depicted in Figure 13: the length of slots L_s , the width of slots W_s , the slot shift from center position S , and the feeding gap F .

Parameter	Value [mm]
L_s	8.94
W_s	2.18
S	1.98
F	3.67

When simulating an antenna in CST, the choice of a proper solver is crucial. Frequency domain solver allowing a tetrahedral meshing with improved accuracy is suitable for the analysis of electrically small structures or devices with a high Q-value. Time domain solver is a general-purpose solver allowing accurate modeling of small and curved structures without the need for local refinement of the mesh [5]. Because of this advantage, the time domain solver was chosen to simulate the performance of the studied antenna.

Reliable analysis is conditioned by proper meshing of the analyzed structure. If the adaptive meshing is selected, the results can be highly accurate, but time of simulation increases significantly. However, such high accuracy is not needed usually.

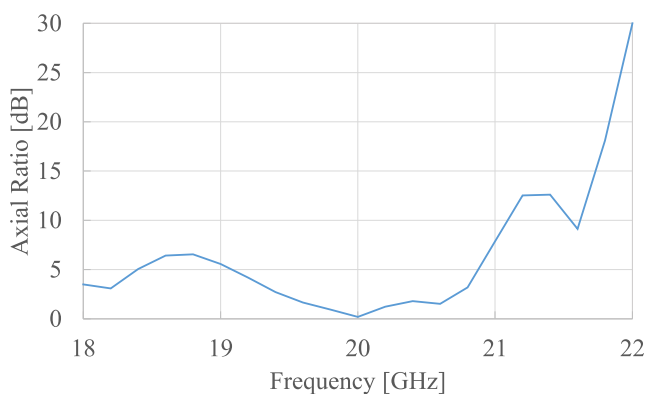


Figure 14: Frequency response of axial ratio of the simulated antenna.

Defining cells per wavelength in global mesh properties allows customizing the density of the mesh. The structure is recommended to be meshed such a way to have 2 to 3 mesh cells between the top and bottom metallization at the port. If this requirement is not fulfilled, an error will appear and the simulation will not start.

Considering the given simulation recommendations, the design of the studied antenna was tuned to obtain satisfactory

frequency response of reflection coefficient, axial ratio, and gain. The values of the parameters of the antenna are given in Table 2.

The axial ratio bandwidth from 19.36 GHz to 20.78 GHz was achieved, which corresponds to 1.42 GHz bandwidth (Figure 14). Simulated directivity pattern of the right handed polarization in 3-D is shown in Figure 15. The gain of the antenna varied from 12 to 14 dBi in the operating bandwidth.

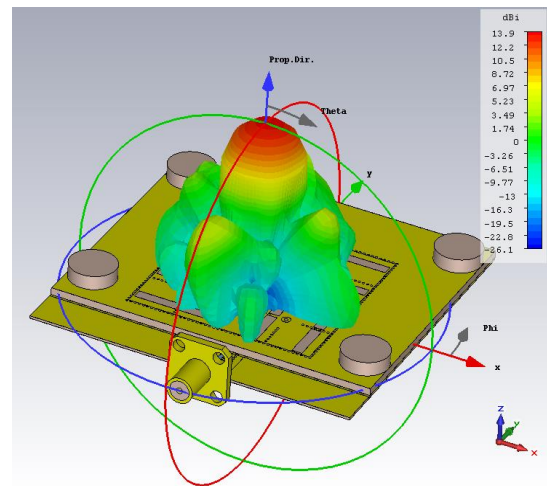


Figure 15: Directivity pattern in 3-D of the simulated antenna

The simulated antenna was manufactured. The alignment of the feeding layer and the radiating one was one of the manufacturing problems. Both the layers have to be well-aligned so that the metal wire can pass through aligned holes and connect the ground metallization and the top one. In order to achieve good alignment of layers, 4 holes were etched on each layer, and plastic screws were used. The manufactured antenna is shown in Figure 16.

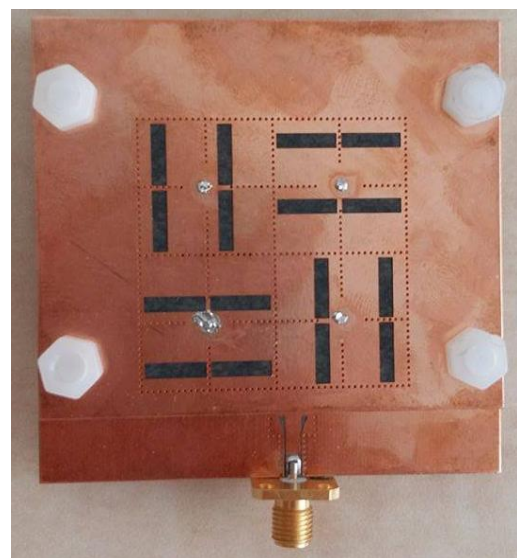


Figure 16: Photograph of the manufactured antenna.

Fabrication of vias through the thicker layer (Arlon Isoclad 933, $h = 1.524$ mm) was identified being an additional problem. In a thicker material, the via is longer in height and a good metallization inside can be hardly achieved. Therefore, some of the vias on the top layer were not metallized properly, and the metallization was needed to be improved.

The bottom layer is very thin, and prone to bending. The layer was slightly bent during cutting and soldering which resulted in a gap between the layers. To overcome this problem, both sides were stuck which connected both layers perfectly. After sticking the layers together, the structure was necessary to be kept under a heavy flat object.

The holes for the wires were requested to be of exactly the same diameter as the available wires. Fitting the wires inside the holes was rather problematic, and therefore, the wires were made slightly thinner. This probably resulted in a slight misalignment of the wires in the holes.

Outputs of measurements of the antenna showed significant deviations from simulated results. Sensitivity analysis to changing parameters was performed in CST Studio. Problems with connecting wires between the layers and lack of metallization in some vias were identified to be the reason of the difference between the measurement and simulation results.

In the sensitivity analysis, the wires were slightly moved from its initial position and metallization of some vias was removed. The frequency response of reflection coefficient of the antenna with changed parameters was similar to the measured reflection coefficient. However, the dependencies are not the same, just experience similar tendencies because not the same vias were lacking metallization and also wires were moved to different positions in the sensitivity analysis as in the manufactured antenna.

Comparison of the frequency response of the reflection coefficient of the simulated and measured antenna and sensitivity analysis antenna is shown in Figure 17.

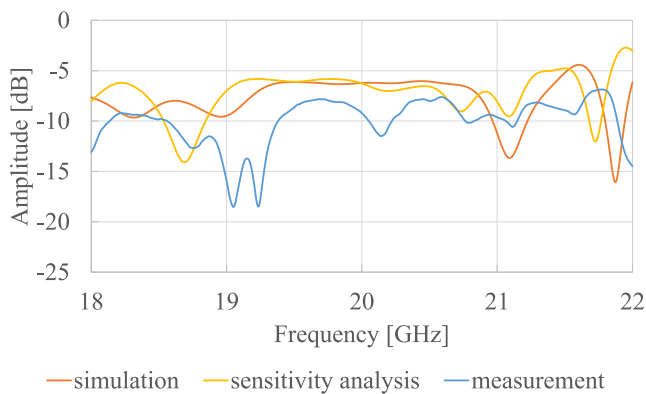


Figure 17: Simulated and measured frequency response of reflection coefficient of the antenna.

Simulated and measured directivity patterns of the antenna for right-handed circular polarization at the central frequency $f = 20$ GHz in the longitudinal plane are shown in Figure 18. The gain of the antenna was not measured, and therefore the radiation patterns are normalized.

4 Summary

In this paper, we present the design procedure of a planar circularly polarized antenna array realized by SIW technology. Designing processes of a SIW, a feeding structure, a radiating structure and a taper were explained in detail. Guidelines for modeling and simulation of the structure in CST Microwave Studio were described. Moreover, problems that the designer might face were discussed together with their solutions.

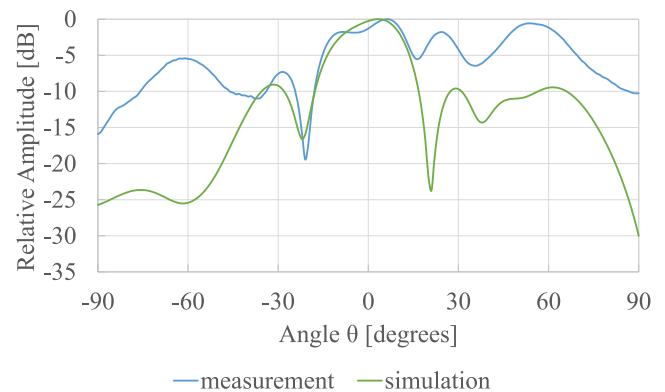


Figure 18: Radiation pattern in the longitudinal cut of the right-handed polarization component (normalized).

Results of the measurements of the antenna were not corresponding with the simulation results because of the manufacturing problems. Sensitivity analysis to changing parameters was performed and the reasons for the disagreement in results were identified. Therefore, we can recommend:

- The use of plastic screws, which can ensure proper alignment of the antenna layer and the feeding one.
- Exploitation of a double-sided sticky tape for fixing the antenna layer and the feeding one together. Thanks to the tape, no air gap between the substrates can appear.
- Selecting thin enough dielectric substrate for the available manufacturing process. That way, problems with a proper metallization of vias can be eliminated.
- Paying attention to misalignment of feeding wires. Alternatively, a different type of feeding is recommended to be used.

Respecting these recommendations can ensure that the studied antenna array can be successfully manufactured.

The paper was written for students and researchers who are starting to develop SIW-based millimeter-wave antennas. We provide practical experience to make the initial design and manufacturing process easier.

Acknowledgement

The published research was funded by the H2020 grant no. 675683 supporting the Innovative Training Network Convergence of Electronics and Photonics Technologies for Enabling Terahertz Applications (ITN CELTA).

References

- [1] Malyuskin, O.; Fusco, V.; Wideband circular polarized antenna with high polarization purity over a wide angular range, 6th European Conference on Antennas and Propagation (EuCAP 2012), p. 2764-2765, DOI: 10.1109/EuCAP.2012.6205905
- [2] Deslandes, D.; Wu, K.; Integrated microstrip and rectangular waveguide in planar form, *IEEE Microwave and Wireless Components Letters*, 2001, vol. 11, no. 2, p. 68-70, DOI: 10.1109/7260.914305
- [3] Deslandes, D.; Wu, K.; Single-substrate integration technique of planar circuits and waveguide filters, *IEEE Transactions on Microwave Theory and Techniques*, 2003, vol. 51, no. 2, p. 593-596, DOI: 10.1109/TMTT.2002.807820
- [4] Huang, J.; A technique for an array to generate circular polarization with linearly polarized elements, *IEEE Transactions on Antennas and Propagation*, 1986, vol. 34, no. 9, p. 1113-1124, DOI: 10.1109/TAP.1986.1143953
- [5] Guan, D.-F.; Ding, C.; Qian, Z.-P.; Zhang, Y.-S.; Guo, J.; Gong, K.; Broadband high-gain SIW cavity-backed circular-polarized array antenna, *IEEE Transactions on Antennas and Propagation*, 2016, vol. 64, no. 4, p. 1493-1497, DOI: 10.1109/TAP.2016.2521904.
- [6] Kim, D.; W. Lee, J.; K. Lee, T.; Sik Cho, C.; Design of SIW Cavity-Backed Circular-Polarized Antennas Using Two Different Feeding Transitions, *IEEE Transactions on Antennas and Propagation* 2011, vol. 59, no. 4, 10.1109/TAP.2011.2109675.
- [7] Abdel-Wahab, W; Wang, Y; Al-Saedi, H; Mohamed, H. A.; Safavi-Naeini, S.; A broadband siw-integrated circular polarized antenna, *IEEE International Symposium on Antennas and Propagation & USNC/URSI National Radio Science Meeting*, 2017, 10.1109/APUSNCURSINRSM.2017.8073208
- [8] Zhang Y.; Cai Y.; Jing N.; Qian Z.; Shi S.; Design of millimeter-wave dual circularly polarized end-fire antenna fed by SIW polarizer, *IEEE MTT-S International Microwave Workshop Series on Advanced Materials and Processes for RF and THz Applications (IMWS-AMP)* 2016, 10.1109/IMWS-AMP.2016.7588387.
- [9] Cassivi, Y.; Perregrini, L.; Arcioni, P.; Bressan, M.; Wu, K.; Conciauro, G. Dispersion characteristics of substrate integrated rectangular waveguide, *IEEE Microwave and Wireless Components Letters*, 2002, vol. 12, no. 9, p. 333-335, DOI: 10.1109/LMWC.2002.803188
- [10] Warmowska, D.; Marek, M.; Raida, Z.; MATLAB-based multi-objective optimization of broadband circularly polarized antennas, *Loughborough Antennas and Propagation Conference (LAPC 2017)*, accepted.
- [11] Deslandes, D.; Design equations for tapered microstrip-to-substrate integrated waveguide transitions, 2010 *IEEE MTT-S International Microwave Symposium*, DOI: 10.1109/MWSYM.2010.5515088
- [12] Kazemi, R.; Sadeghzadeh, R.A.; Fathy, A.; A new compact wide band 8-way SIW power divider at X-band, *Loughborough Antennas and Propagation Conference (LAPC 2011)*, DOI: 10.1109/LAPC.2011.6114098